Journal of Aerosol Science
Volume 40, Issue 10, October 2009, Pages 833-843

MEASUREMENTS OF THE TEMPERATURE DEPENDENT DIFFUSION COEFFICIENT OF NANOPARTICLES IN THE RANGE OF 295 TO 600 K AT ATMOSPHERIC PRESSURE

V. Ya. Rudyak[1,2], S. N. Dubtsov [3], A. M. Baklanov[3]

1 – *Novosibirsk State University of Architecture and Civil Engineering, Leningradskaya str., 113, 630008, Novosibirsk, Russia*
2 – *Baker Hughes Inc., Kutateladze str., 4a, 630090, Novosibirsk, Russia*
3 – *Institute of Chemical Kinetics and Combustion of the Siberian Branch of the Russian Academy of Science, Institutskaya str., 3, 630090, Novosibirsk, Russia*

Corresponding author: Valery Ya. Rudyak, – *Novosibirsk State University of Architecture and Civil Engineering, Leningradskaya str., 113, 630008, Novosibirsk, Russia*
e-mail: valery.rudyak@mail.ru

ABSTRACT

The diffusion coefficient of WOx, Pt and NaCl particles in the diameter range of 3 to 84 nm was determined from the penetration of a set of wire screens in the temperature range of 295 to 600 K. The temperature dependence could be approximated well by a power law $D \sim T^{\alpha}$, where α decreases from 1.7 to 1.55 with increasing particle diameter. This dependence differs significantly from the predictions of various correlations, and in particular the Cunningham-Millikan-Davies (CMD) correlation. A modification to the CMD correlation is suggested which includes temperature dependent empirical coefficients.

KEYWORDS

Diffusion coefficient temperature dependence, nanoparticles, ultra-fine aerosol particles, diffusion battery, CMD-correlation

1. Introduction

Diffusion of aerosol and colloid particles is an important factor in their evolution and hence has been actively researched throughout the second half of the last century. Experimental investigations of the nanoparticles diffusivity have been the subject of many research efforts. One of the most widely used methods for the determination of the diffusion coefficient is the measurement of nanoparticle deposition in various diffusion batteries (DB). The detailed description of various types of DB, as well as the results of the nanoparticle diffusion investigations, is presented by Knutson, (1999) and Cheng (1993). Pedder (1971) reports on the diffusion coefficient measurement for 3÷10 nm sized aerosol particles, based on the measurement of their deposition in a rectangular channel DB at room temperature. The measurement of the diffusivity of soot clusters of 10÷20 nm in size with a DB is described by Clary (1988). Alonso et al. (1997) have investigated nanoparticle penetration through wire screens and laminar flow tubes at room temperature, too. The results of above-sited papers are in good agreement with CMD calculations. The particle penetration was shown to be well described by the fan model (Chen, 1980) for the particles above 2 nm in diameter. Penetration of the singly-charged particles was found to be the same as for uncharged particles. King et al. (1983) report on the measurements of soot nanoparticle diffusion in flame by means of photon-correlated spectroscopy. The measured values for diffusion coefficients differed significantly from those calculated from CMD-correlation. On the other hand, the diffusion coefficients of soot particles in flame, measured using the dynamic light-scattering method agree well with the calculations according to the kinetic theory (Flower, 1983).

As of today, a number of effective experimental methods aimed at measuring the diffusion coefficient and the sizes of aerosol particles have been developed (such as diffusion batteries, differential analyzer of electric mobility, etc.). The Einstein formula below for the diffusion coefficient of the Brownian particles has been the theoretical basis for most of these methods of measurement

$$D_E = kT / \gamma_S , \qquad \gamma_S = 6\pi\eta R , \tag{1.1}$$

Here η and T are the viscosity coefficient of the carrier medium and its temperature, respectively, R is the characteristic radius of the particle.

Formula (1.1) contains the drag coefficient γ_S; this is the drag coefficient corresponding to the Stokes drag force applied to the spherical particle in a non-compressible fluid. To expand the applicability range of formula (1.1) and make it valid for describing diffusion of dispersed particles in a rarified gas, the so called Cunningham–Milliken–Davies correlation (CMD) is commonly used (Friedlander, 2000)

$$D_c = kT / \gamma_c , \quad \gamma_c = 6\pi\eta R\left[1 + AKn + QKn\exp(-b / Kn)\right]^{-1} = 6\pi\eta R / C , \tag{1.2}$$

where A = 1.257, Q = 0.4, b = 1.1, $Kn = l / R$ is the Knudsen number based on the particle radius, l is the free path length of the carrier gas molecules. Equation (1.2) is widely used in different applications. Moreover, it is introduced instrumentally into a number of methods of evaluating the aerosol particle size and their diffusion coefficients (Knutson, 1999; Koutsenogii, 1987).

There are some attempts to describe the diffusion of aerosol particles by means of the kinetic theory. The first formula for diffusion coefficient was obtained by Epstein (Epstein, 1924; see also review Mädler and Friedlender, 2007) for case large Knudsen

numbers. Later the approximate solutions for the drug force acting on aerosol particle in gas at smaller Knudsen numbers was built in paper (see Philips, 1975 and references cited there). Using the Einstein relation it is possible to obtain respective diffusion coefficient. However, all mentioned formulas are practically semi-empirical because they include the accommodation coefficients. The latest are the function of the material of the particles and type of carrier gas. In addition they depend on temperature of gas and in general on size of nanoparticles and their form.

The Chapman – Enskog solution of the Boltzmann equations gives known formula for the diffusion coefficient of binary mixtures (Chapman and Cowling, 1970) $D_{12} = 3\sqrt{2\pi m_{12} kT}\,/(16 n\pi\sigma^2\Omega)$, where $m_{12} = (m_1 + m_2)/m_1 m_2$, m_i – molecules masses, k – Boltztmann constant, T – temperature, n – career gas density, σ – collision diameter of molecules, Ω – so named collision integral. From this formula the simple estimate follows: $D_{12} \sim T^{3/2}/\Omega(T)$. The temperature dependence of diffusion coefficient is defined not only by $T^{3/2}$, but by the temperature dependence of Ω-integrals also. This last depends on the intermolecular potential. The transport processes of nanoparticles in rarefied gases are well described by the Boltzmann equation (Rudyak and Krasnolutskii, 2001, 2002a). However the interaction of nanoparticle with carrier gas molecules is not local. The colliding molecule interacts simultaneously with all atoms (or molecules) of nanoparticle. Such interaction is described by the special potential which was constructed in paper (Rudyak and Krasnolutskii, 1999). It was shown (Rudyak and Krasnolutskii, 2001, 2002a) that depending on size of the particles the value of the Ω-integral in the mentioned above formula can change by two-three times.

It was shown in kinetic theory (Rudyak and Krasnolutskii (2001, 2002a) that correlation (1.2) does not describe diffusion of fairly small nanoparticles. Later these results were confirmed experimentally by Rudyak et al., (2002b). Furthermore, it was established that, even for larger particles, correlation (1.2) is valid only in a very narrow temperature domain. This is not surprising as the parameters contained in this correlation were determined within a narrow temperature range (19÷24 °C). For this reason, dependence of the diffusion coefficient both for nanoparticles and larger particles should differ considerably from dependences predicted by formulae (1.1) and (1.2).

The objective of the present paper is to study temperature dependence of the diffusion coefficient for nanoparticles experimentally. The data given here were obtained for nanoparticles of WO_x (actually, these particles are made of WO_3 with a small admixture of WO_2), NaCl and Pt. The particle diameter ranged between 3 and 100 nm, and temperature ranged from 295 to 650 K.

2. Experimental Setup and Method of Measurement

Experimental setup is shown in Fig. 1. A flow of air or nitrogen used in these experiments was purified by the BOG-85 purification module (it is marked by the digit 1 in the diagram). The module consists of three consecutively connected columns filled with absorbents (SiO_2, activated carbon, 13X molecular sieve) which remove H_2O, NH_3, CO, hydrocarbons, and other impurities from the air. The purified gas flow was supplied to the aerosol generator 3. The Q_1 value was controlled by the flow meter 2; and was varied

from 0.1 to 0.3 l/min. The particle flow at the exit from the generator was diluted by the pure gas flow Q_2 up to 1.1 l/min.

The aerosol particles were supplied via a three-way valve 5 (see Fig. 1) to holders 6 and 7. In one of the holders, perpendicular to the gas flow, a set of screens was inserted, whereas the other remained empty. Two screen types were used in the experiments. The first type was made of wire with thickness d_w = 100 μ, the cell dimensions were 123×123 μm×μm. The second type was made of wire with thickness d_w = 200 μ, the cell dimensions were 250×250 μm×μm. Depending on the particle size, the number of screens in the holder varied from 3 to 15, it was selected so that, at room temperature, 40 – 50 % of the particles with a given size deposited on the screens. The carrier gas flux through the holders (Q_1+Q_2) in all the experiments varied from 1.1 to 1.3 l/min.). The flux Q_4 of 1.0 l/min was supplied to Novosibirsk-type Automated Diffusion Battery (NADB, see module 9 in Fig. 1), and excess air Q_3 was emitted into the vent via the aerosol filter 4.

Concentration of aerosol particles which passed through the holders, and their size distribution, were measured by NADB (Ankilov, 2002). NADB consists of 8-stages screen-type diffusion battery, turbulent mixing-type condensation enlarger with DBP as a working substance, photoelectrical particle counter and programmable interface controller. A personal computer was used for controlling the exchange, storage, and processing of measurement data (10 in Fig. 1). The NADB enabled us to measure the concentration of aerosol particles and their size distribution within the ranges from 5 to $3\cdot10^5$ particles/cm^3 (without dilution) and from 3 to 200 nm, respectively.

Holders and feeding tubes were placed in the thermostat. In these experiments, we used the thermostat of the "Tsvet-100" gas-liquid chromatograph (T = 20÷350^o C). To connect modules of the experimental setup to each other, stainless steel tubes with the inner diameter d_{inn} = 3 mm and outer diameter d_{out} = 4 mm were employed.

A Collisson-type nebulizer (Green and Lane, 1964) and a "hot-wire" generator of WO_x nanoparticles (Baklanov and Dubtsov, 1993) were used to produce nanoparticles of the desired size and concentration. The operational principle of the latter is as follows: a flow of air is forced through an incandescent tungsten wire, the surface layer of the wire oxidizes, and resulting tungsten oxide vaporizes. After cooling down, this vapor condenses producing WO_x ($x \approx 2.9$) nanoparticles. Depending on wire temperature and air flows Q_1, Q_2, the size and concentration of these particles can be varied from 2 to 20 nm in diameter, and from 10^4 to 10^7 particles/cm^3 respectively. Stability of the size and concentration of these particles is ± 5 % for the period of 4 hours in the whole temperature range.

In addition to these generators, a high-frequency spark discharge generator with Pt electrodes, similar to that, described in (Schwyn et al., 1988; Horvath and Gangl, 2003) was used to produce nanoparticles of platinum. In this case, instead of air, nitrogen was used as a carrier gas. Platinum wire of 0.2 mm in diameter was used for electrodes; the electrodes were spaced at 1 mm. The sparking frequency varied from 0.6 to 3.6 kHz, and the nitrogen flux Q_1 ranged between 0.1 and 0.5 l/min. By changing the sparking frequency and flux Q_1, we were able to obtain particles of different diameters in the range from 6 to 55 nm, with concentration up to 10^7 particle/cm^3.

The experimental procedure of measuring of aerosol particles penetration through the screens consisted of several steps. After the necessary temperature was established

inside the thermostat, the flow of aerosol particles was directed via the three-way valve 5 (Fig. 1) to the empty holder. Next, the size distribution and concentration of these particles were measured three times consecutively. Then, only total concentration was measured 10 times. After that, the valve 5 was turned to another position to redirect the flow of particles to the screens-containing holder 7. Here, again, total concentration of particles which passed through the set of screens was measured 10 times. This procedure was repeated five times. Finally, the size distribution and concentration of particles were once again measured three times. The variation of the particles mean diameter did not exceed ± 5% in the whole temperature range for all nanoparticles, used in the experiments. The penetration P of nanoparticles passing through the nets was found as the ratio of the average concentration c of particles which passed through the holder with nets to the average concentration c_0 of particles which passed through the empty holder.

3. Accuracy of Measurement and Method of Experimental Data Interpretation

The diffusion coefficient was determined from measured values of the penetration using the procedure suggested in (Chen and Yeh, 1980) as follows

$$D = \left(-\ln P / \gamma S\right)^{3/2}. \tag{3.1}$$

Here $S = 4\alpha h\left[\pi(1-\alpha)d_w\right]^{-1}$, $\gamma = 2/7n(ud_w)^{-2/3}$, and α is the solid volume fraction of the screen, h is thickness of the screen, d_w is wire thickness, n is the number of screens, u is the face velocity. In this model it is supposed that sticking coefficient of nanoparticle is equal to unity. It seems, that this coefficient may decrease with the gas temperature increase. However, Shin et al. (2008) did not detect thermal rebound for 3÷20 nm sized nanoparticles in the temperature range up to 500 K. Therefore we considered that sticking probability of the particles equals to unity and does not change with temperature increase.

Equation (3.1), by itself, does not allow us to link the diffusion coefficient with the size of the particles under study. To match particle radii with corresponding diffusion coefficients, the CMD correlation is used (1.2). As a result, the particle radius is found as follows

$$R = \frac{kTC}{6\pi\eta}\left[-\frac{\gamma S}{\ln P}\right]^{3/2}. \tag{3.2}$$

For this reason, verification of the method of determining the nanoparticle size appeared very important. To this end, monodispersed latex particles were employed. Typical results obtained are shown in Fig. 2. There one can see three histograms of experimentally found distributions for three sizes of latex particles. Latex particles are spherical, and their size is determined by their diameter d_p. In Fig. 2, distributions for particles of diameters d_{p1} = 41 ± 1.2 nm, d_{p2} = 60 ± 3.6 nm, and d_{p3} = 100 ± 5 nm are given. Approximations of these histograms with log-normal distributions, as follows

$$F\left(d_p\right) = \frac{1}{\sqrt{2\pi \ln^2 \sigma_g}} \exp\left\{-\frac{\ln^2\left(d_p/d_g\right)}{2\ln^2 \sigma_g}\right\} \tag{3.3}$$

correspond to curves 1, 2, and 3. In formula (3.3) d_g is the mean geometric particle diameter, and σ_g is the geometric standard deviation of particle diameter.

As a result of measurements, the following data were obtained: d_{p1} = 37±2 nm, d_{p2} = 63±4 nm, d_{p3} = 99±6 nm. It should be noted, however, that when latex is sprayed, small particles in the range from 5 nm to 20 nm are formed as well (these are formed from the solvent, i.e. deionized water). The spectrum of these particles formed due to spraying of deionized water was subtracted from the spectrum of latex particles. Thus, measured mean diameters of latex particles coincide with instrument ratings with a 10% error. It can be shown that the diffusion coefficient is found with similar accuracy.

Examples of particle size distributions, for WO_x, Pt and NaCl particles, used in our experiments, are given in Fig. 3. Here the points are the experimental data and lines are their approximation by the log-normal curves (3.3).

At room temperature, our data on the diffusion coefficient agree well with CMD correlation (1.2), experimental results published by other authors, and existing correlations. This agreement can be observed in Fig. 4. Here, together with correlation (3.1), data from (Baron and Willeke, 2001; Dubtsov et al., 2005; Reid et al., 1977) are also given. In all cases gas temperature was the same, T = 295 ± 2 K.

4. Measurement Results

As it was mentioned above, we measured the penetration P experimentally. Temperature dependence typical of this coefficient is shown in Fig. 5 for 3.7 nm WO_3 nanoparticles (filled squares). As temperature increases, the penetration decreases. On the other hand, according to (3.1), the penetration decrease with the temperature increase means also the increase in the diffusion coefficient. It is this relationship that is shown in Fig. 5 where temperature dependence of the diffusion coefficient for nanoparticles is marked with opened circles.

The goal of the present paper is to study temperature dependence of the diffusion coefficient for nanoparticles experimentally. The difficulties in solving this problem were related to the following tasks:

- It was necessary to study this dependence within a wide range of temperatures;
- It was necessary to study this dependence within a wide range of sizes of aerosol particles;
- It was necessary to study this dependence for particles of the same size but made of different materials.

In this section, the portion of experimental data that we deem most typical of measuring the diffusion coefficient for nanoparticles is given. Experimental results are presented in Tables 1 – 2.

The data obtained were compared with the data calculated using the CMD correlation (1.2) and experimental correlation (Baron and Willeke, 2001). As it was shown above (see Fig. 4), all correlations describe experimental data perfectly at room temperature. However, this agreement disappears with the increase of temperature. Fig. 6 shows comparison between experimental data (filled circles), CMD correlation (dashed line), the correlation from (Baron and Willeke, 2001) (dotted line) with respect to temperature dependence of the diffusion coefficient for 10±1 nm WO_3 nanoparticles in air. Both correlations appear inapplicable at temperatures above 350 K. At the temperature of 620 K,

the experimentally measured diffusion coefficient equals double the value given by the CMD correlation. A similar situation is observed for other nanoparticles. Fig. 7 shows temperature dependence of the diffusion coefficient for Pt nanoparticles in nitrogen, the diameter of nanoparticles being 18±2 nm.

Finally, it should be noted that neither the CMD correlation, nor the correlation from Baron and Willeke (2001) enables us to correctly describe temperature dependence of the diffusion coefficient for both nanoparticles and Brownian particles. In particular, this can be seen from comparison between experimental data and those computed using the correlations shown in Fig. 8 (notations being the same as in Fig. 7). In this Figure, temperature dependence of the diffusion coefficient for 84 nm NaCl particles is presented.

5. Regarding Modification of CMD correlation.

The fact that the CMD correlation (1.2) is widely spread and successfully applied can be explained by two factors. First, it has the Einstein formula (1.1) as the basis, and secondly, it agrees well with the free molecular asymptotic value of the drag force applicable at $Kn >> 1$. However, its parameters were determined within a narrow temperature range, and thus, it is valid only in a very narrow domain. The previous section of the present paper has demonstrated this weakness clearly. On the other hand, the CMD correlation is designed quite sensibly and, as it was shown above, fits several limit asymptotic values. For this reason, it could be used for developing a more general correlation, applicable within a wide temperature range. In order to make the correlation (1.2) applicable within a wide temperature range, we modify it as follows

$$D_k = kT/\gamma_k, \quad \gamma_k = 6\pi\eta R\left[1 + A^* Kn + Q^* Kn\exp(-b/Kn)\right]^{-1} \tag{5.1}$$

so that its parameters become functions of temperature

$$A^* = A(T/295)^j, \quad Q^* = Q(T/295)^j. \tag{5.2}$$

There are formal foundations for this modification. Indeed, one could show that parameters A and Q in (1.2) are related to the choice of certain accommodation coefficients. The latter is a function of temperature, and in this case relationship (5.2) is well justified.

Temperature dependence of the diffusion coefficient for Brownian particles (1.1) is determined by corresponding changes in viscosity of the carrier medium and turns out fairly weak. It can be shown (Rudyak, 2002a) that in this case $D_E \sim T^{0.35}$. On the other hand, molecular diffusion grows with temperature at a much greater rate: $D \sim T^{\alpha}$, where the power index α depends on the substance and ranges from 1.6 for UF_6 to 1.92 for oxygen and argon. Thus, power law dependence (5.2) also appears logical. At the same time, one should expect that the parameter j will not be universal. It may depend on (i) nanoparticle material, (ii) nanoparticle size.

As for the first dependence, it was shown in our paper (Rudyal et al., 2008) that it is fairly strong for nanoparticles with characteristic diameter $d_p \le 5 \div 10$ nm. Moreover, taking into account nanoparticle material seems to have differing effects on transfer properties. For instance, our experiments show that, starting with sizes of 6 nm and up, nanoparticle material properties have little influence on the diffusion coefficient. Fig. 9

provides a good illustration to that: temperature dependences of the diffusion coefficient for 6.3 nm *Pt* nanoparticles in nitrogen and for 6.2 nm WO_x nanoparticles in air are compared. The data obtained appear to agree well in the entire temperature domain with accuracy up to the measurement error. Thus, for not-so-small nanoparticles, the parameter *j* does not have any significant dependence on their material.

Let us consider the character of temperature dependence of the diffusion coefficient for nanoparticles of various sizes. Comparison of these dependences for molecules and Brownian particles points to a possible character of temperature dependence of the diffusion coefficient; it appears that the following equation should be true

$$D \sim T^n \tag{5.3}$$

where $n > 0.35$, but $n < 2$. The experiments performed seem to confirm this opinion. It was established that for particles with diameters smaller than 10 nm, $n \sim 1.7 \pm 0.2$. With the increase of the diameter, the value of *n* somewhat decreases, and for 84 nm particles it reaches 1.49 ± 0.12.

Now, let us go back to correlations (5.1)–(5.2). For not-so-small nanoparticles, the *j* parameter does not seem to have any significant dependence either on their material or on the carrier gas. Systematic measurements yielded its value for a number of discrete values of nanoparticle diameters. Indeed, the *j* parameter depends on the nanoparticle size. For 8.7 nm nanoparticles it is 0.95; for 18 nm nanoparticles, 1.05; for 84 nm nanoparticles, also 1.05. Thus, as the nanoparticle size increases, the *j* parameter quickly reaches a certain constant value. This enables us to suggest a fairly simple formula for finding the *j* parameter

$$j = 1.03 + \frac{0.57}{1 + 10^{d_p/0.37 - 10.45}}, \tag{5.4}$$

where d_p is the nanoparticle diameter in nanometers. Fig. 10 compares formula (5.4) with experimental data.

Conclusion

Systematic measurements performed enable us to draw a predictable conclusion the diffusion coefficient of aerosol particles strongly depends on the carrier gas temperature. It should be emphasized that diffusion of the Brownian particles in liquid, described by the Einstein formula (1.1), depends on temperature through changes in carrier liquid viscosity only. The character of this dependence is the same for particles of different sizes and made of different materials. The CMD correlation (1.2) yields a more complex temperature dependence of the diffusion coefficient. Here temperature dependence of the diffusion coefficient is determined by two factors. First, just as in the Einstein formula, it is determined by temperature dependence of the viscosity coefficient of the carrier gas. Besides, the free path length for the gas molecules, which is contained in the Knudsen number, is a function of temperature, too. On the other hand, the CMD correlation predicts the same character of such dependence for all particles of a given size (regardless of their material, density, etc.).

One of the possible reasons for the discrepancy between experimental results and CMD correlation could be particle charging at elevated temperatures. The decrease in penetration will result in the higher value of the diffusion coefficient, calculated from

particles penetration. In our experiments nanoparticles were generated by three different methods. NaCl particles were generated by Collisson atomizer. There are practically no reasons for these particles to be charged. Therefore the particle charge plays no role in this case. However, we obtained qualitatively the same results for all particles (NaCl, Pt, WO_x).

We cannot exclude the possibility that some fraction of the aerosol particles, used in our experiments, could be naturally charged during their generation. If the fraction of these particles increases with temperature, this fraction will remain the same after cooling, at least for some time. This additional charging will lead to the experimentally measured higher value of the diffusion coefficient and, as a result, to a lower value for the aerosol particles diameter. Nevertheless, our experiments showed that the particles diameter was constant within ± 5% and did not depend on temperature (see section 2). So, we assume that there is no additional particle charging in our experiments.

The present paper has shown experimentally that neither the CMD correlation, nor any other correlation known to the present authors is able to yield correct temperature dependence of the diffusion coefficient for aerosol particles. These correlations work at room temperature only. At high temperatures, real values of the diffusion coefficient for aerosol particles observed in the experiments differ from correlation (1.2) values by several times. It had been predicted earlier by the kinetic theory (Rudyak, 2001; 2008), so the results were, in this sense, expected.

Experiments showed that the character of temperature dependence of the diffusion coefficient for aerosol particles, in the general case, is determined by the size and material of the particles. This dependence is stronger for smaller particles. Dependence on material is negligible for particles greater than 6 nm in diameter. However, for very small nanoparticles, this dependence becomes a key factor.

Modification of the CMD correlation (5.1)–(5.2) suggested in the present paper seems to describe our experimental results fairly well, and it could be used in practical applications. However, it should be noted that accuracy of our experimental data does not exceed 10%. Therefore, one cannot expect better accuracy when using correlation (5.1)–(5.2) as well. It might be beneficial to perform experiments (i) with the highest possible accuracy and (ii) using an alternative method of measuring the diffusion coefficient, e.g. the method of measuring electric mobility (the DMA method).

One ought to exercise caution when using the modified CMD correlation for very small particles with characteristic sizes smaller than 10 nm. As it was shown in (Rudyak, 2002b), the method of recovering the nanoparticle size by means of the CMD correlation (2) via measuring nanoparticle electric mobility produces a 20–30% error. The DMA method gives exaggerated values of nanoparticle diameters. The same is true about the diffusion batteries method. For this reason, it may be beneficial to perform systematic measurements of temperature dependence of the diffusion coefficient for nanoparticles, additionally controlling nanoparticle sizes by means of the electronic microscope and correcting formula (5.2) in the process.

Of course, it would be advantageous to perform experiments in a wider temperature range. In particular, it could be interesting to cover the low temperature range. Understandable experimental problems would arise here: e.g. we would not be able to perform experiments in air. It would also be important to widen the variety of nanoparticle materials and carrier gases.

Finally, it should be emphasized that we performed all our experiments at normal pressures. In this case, the free path length for carrier gas molecules was about $10^{-4} \div 10^{-5}$ cm. For Brownian particles, the Knudsen numbers turned out to be about unity or even greater. However, the Knudsen numbers we have for nanoparticles are all small or even very small. In spite of that, the drag force applied to these particles would not be described by the Stokes law, and the diffusion coefficient would not be described by the Einstein formula (1.1). The kinetic theory should be employed to describe diffusion in this case.

Acknowledgments

This work was supported in part by the Russian Foundation for Basic Research (grant No. 07-08-00164) and the grant of support of the leading scientific schools (grant No. NSh-454.2008.1).

References

Alonso, M., Kousaka, Y., Hashimoto, T., & Hashimoto, N. (1997). Penetration of nanometer-sized aerosol particles through wire screen and laminar flow tube. *Aerosol Science and Technology*, *27*, 471–480.

Ankilov, A.N., Baklanov, A.M., Colhoun, M., Enderle, K.-H., Gras, J., Julanov, Yu., Kaller, D., Lindner, A., Lushnikov, A.A., Mavliev, R., McGovern, F., Mirme, A., O'Connor, T.C., Podzimek, J., Preining, O., Reischl, G.P., Rudolf, R., Sem, G.J.,. Szymanski, W.W., Tamm, E., Vrtala, A.E., Wagner, P.E., Winklmayr, W., & Zagaynov, V. (2002). Intercomparison of number concentration measurements by various aerosol particle counters. *Atmospheric Research, 62*, 177–207.

Baklanov, A.M., & Dubtsov, S.N. (1993). An experimental set-up for aerosol spectrometers calibration. *Journal of Aerosol Science, 24, Supplement 1*, S237–S238.

Baron P.A., & Willeke K. (Eds.) 2001. *Aerosol Measurement: Principles, Techniques, and Applications*. New York: Wiley.

Chapman, S., and Cowling, T.G. (1970). *The Mathematical Theory of Non-Uniform Gases.* Cambridge: Cambridge University Press.

Cheng, Y.S., & Yeh, H.C. (1980). Theory of a screen-type diffusion battery. *Journal of Aerosol Science, 11,* 313–320.

Cheng, Y.S. (1993). Condensation detection and diffusion size separation techniques. In *Aerosol Measurement: Principles, Techniques, and Applications.* Baron, P.A., & Willeke, K., (Eds.). Van Nostrand Rheinhold: New York, Chapter 19.

Clary T., Mulholland, G., & Gentry, J.W. (1988). The experimental measurement of clusters formed from soot agglomerates near the sooting limit. *Lecture Notes in Physics, 309*, 120–123.

Dubtsov, S.N., Dultsev, E.N., Ankilov, A.N., Levykin, A.I., & Sabelfeld, K.K. (2005). Kinetics of aerosol formation during tungsten hexacarbonyl photolysis at reduced pressure. *Chimicheskaya Fizika (in Russian)*, *24,* 89–95.

Flower, W.L. (1983). Measurement of the diffusion coefficients for soot particles in flames. *Physical Review Letters, 51,* 2287–2290.

Friedlander, S.K. (2000). *Smoke, dust, and haze. Fundamentals of aerosol dynamics*. Oxford: Oxford University Press.

Garwin E., Schwyn S., & Schmitdt-Ott, A. (1988). Aerosol generation by spark discharges. *Journal of Aerosol Science*, *19,* 639–642.

Green, H. & Lane, W. (1964). *Particulate Clouds: Dust, Smokes and Mists,* second ed., London: Spon Ltd.

Horvath, H., & Gangl, M. (2003). A low-voltage spark generator for production of carbon particles. *Journal of Aerosol Science, 34,* 1581–1588.

King, G.B., Sorensen, C.M., Lester, T.W., & Merklin, J.F. (1983). Direct measurements of aerosol diffusion constants in the intermediate Knutsen regime. *Physical Review Letters, 50,* 1125–1128.

Knutson, E. O. (1999). History of diffusion batteries in aerosol measurements. *Aerosol Science and Technology. 31,* 83–128.

Koutsenogii, K.P. (1987). Methods of aerosol particles' concentration and size determination. *Analytical review No 4393*. Moscow: Central Research Institute of Information and Technical-economical Research (in Russian).

Mädler, L. & Friedlender, S.K. (2007) Transport of nanoparticles in gases: overview and recent advances. *Aerosol and Quility Reseach, 7*, 304–342.
Pedder, M.A. (1971). The measurement of size and diffusion characteristics of aerosols with particle size less than 0.01 μm using Polak condensation nucleus counter. *Journal of Physics, D: Applied Physics, 4,* 531–538.
Phillips, W.F. (1975). Drug on a small sphere moving through a gas. *Phys. Fluids, 18*, 1089–1093.
Reid, R.C., Prausnitz, J.M., & Sherwood, T.K. (1977). *The properties of gases and liquids.* Third ed. New York: McGraw-Hill.
Rudyak, V.Ya., & Krasnolutskii, S. L. (1999). The interaction potential of dispersed particles with carrier gas molecules. In *Rarefied Gas Dynamics XXI. Proc. 21st Int. Symp. on RGD*. V. I. Gepadnes-Editors. P. 264–270.
Rudyak, V.Ya., & Krasnolutskii, S.L. (2001). Kinetic description of nanoparticles diffusion in rarefied gases. *Russian Physical Dokl. (USA), 46,* 1336–1339.
Rudyak V.Ya., & Krasnolutskii, S.L. (2002a). Diffusion of Nanoparticles in a Rarefied Gas. *Technical Physics, 47,* 807–813.
Rudyak, V.Ya., Krasnolutskii, S.L., Nasibulin, A.G., & Kauppinen, E.I., (2002b). About measurement methods of nanoparticles sizes and diffusion coefficient. *Doklady Physics, 47,* 758–761.
Rudyak, V.Ya., Krasnolutskii, S.L., & Ivaschenko E.N. (2008). On the influence of the physical properties of nanoparticles material on their diffusion in rarefied gas. *Journal of Engineering Physics and Thermophysics, 81*. 76–81 (in Russian).
W.G. Shin, G.W. Mulholland, S.C. Kim, and. Pui, D.Y (2008). Experimental study of filtration efficiency of nanoparticles below 20 nm at elevated temperatures. *J. Aerosol Science*, *39*, 488-499.

Figure captions

Figure 1. Schematic of the experimental set – up . 1 – gas purification unit "BOG-85", 2 – flow meters, 3 – "hot-wire" generator of WO_x nanoparicles, 4 – HEPA filter, 5 – three-way stopcock, 6 – empty holder, 7 – holder with screens, 8 – thermostat, 9 – NADB, 10 – PC, Q_1, Q_2, Q_3 – career gas flows.

Figure 2. Normalized size distributions of polystyrene latex particles, produced with Colisson-type nebulizer. Size distributions were normalized in a way, that amplitudes of the size distributions maxima had similar values. The types of latex particles has been used: 1 – 41 ± 1.2 nm, 2 – 60 ± 3.6 nm, 3 – 100 ± 5 nm (manufacture's information).

Figure 3. An example of the size distributions of the aerosol particles used in experiments. WO_x – tungsten oxide particles with mean arithmetic diameter of 3.7 and 12.1 nm, Pt – platinum particles with mean arithmetic diameter of 34.5 nm, NaCl – NaCl particles with mean arithmetic diameter of 84 nm. Dots – data, measured with NADB, lines – log-normal fit.

Figure 4. Comparison of the experimentally measured diffusion coefficients (1) for WO_3, Pt and NaCl nanoparticles of different size with calculated values. 2 – CMD-correlation (2), 3 – Baron and Willeke (2001), 4 – experimental correlation (Dubtsov,2005), 5 – Chapman equation (Reid, 1977)

Figure 5. Temperature dependence of the penetration (closed squares) and diffusion coefficient (open circles) for 3.7 nm WO_x nanoparticles in air.

Figure 6. Comparison of the experimentally measured diffusion coefficient temperature dependence of WO_x nanoparticles in air (1) with calculations using CMD-correlation (2) and formulae in (Baron and Willeke, 2001) (3). Line – approximation $D \sim T^{1.7}$. Mean arithmetic diameter of the nanoparticles – 3.5 nm.

Figure 7. Comparison of the experimentally measured diffusion coefficient temperature dependence of Pt nanoparticles in nitrogen (1) with calculations using CMD-correlation (2) and formulae in (Baron and Willeke, 2001) (3). Line – approximation $D \sim T^{1.55}$. Mean arithmetic diameter of the nanoparticles – 18 ± 2 nm.

Figure 8. Comparison of the experimentally measured diffusion coefficient temperature dependence of NaCl nanoparticles in air (1) with calculations using CMD-correlation (2) and formulae in (Baron and Willeke, 2001) (3). Line – approximation $D \sim T^{1.40}$. Mean arithmetic diameter of the nanoparticles – 84 ± 6 nm.

Figure 9. Diffusion coefficient temperature dependence for 6.3 nm WO_x in air (filled circles) and 6.2 nm Pt nanoparticles in N_2 (opened circles).

Figure 10. Dependence of the exponent *j* value in the formulae (5.4) on the particle's size.

Table 1. Experimentally measured values of the diffusion coefficient D for WO_x nanoparticles with mean arithmetic diameter of 3.5, 4.4, 6.2, 7.6, 8.7 and 10.0 nm.

d = 3.5 nm		d = 4.4 nm	
T, K	D, cm^2/s	T, K	D, cm^2/s
294.7	$4.76\times10^{-3}\pm1.07\times10^{-3}$	296	$2.97\times10^{-3}\pm2.43\times10^{-4}$
325.2	$8.14\times10^{-3}\pm5.22\times10^{-4}$	313.2	$4.27\times10^{-3}\pm3.24\times10^{-4}$
367.2	$1.21\times10^{-2}\pm7.73\times10^{-4}$	338.2	$5.28\times10^{-3}\pm4.75\times10^{-4}$
417.2	$1.53\times10^{-2}\pm1.66\times10^{-3}$	379.3	$5.33\times10^{-3}\pm4.91\times10^{-4}$
459.6	$1.89\times10^{-2}\pm1.30\times10^{-3}$	401.5	$5.94\times10^{-3}\pm1.41\times10^{-4}$
517.8	$2.45\times10^{-2}\pm2.14\times10^{-3}$	438.1	$7.45\times10^{-3}\pm2.42\times10^{-4}$
		483.2	$9.01\times10^{-3}\pm7.06\times10^{-4}$
		514.2	$1.04\times10^{-2}\pm8.63\times10^{-4}$
		573.5	$1.32\times10^{-2}\pm1.27\times10^{-3}$
d = 6.2 nm		d = 7.6 nm	
295.16	$1.41\times10^{-2}\pm1.40\times10^{-4}$	298	$8.70\times10^{-4}\pm3.27\times10^{-5}$
334.16	$1.95\times10^{-2}\pm3.27\times10^{-4}$	319.2	$9.91\times10^{-4}\pm3.33\times10^{-5}$
384.16	$2.69\times10^{-2}\pm8.75\times10^{-4}$	366.2	$1.17\times10^{-4}\pm8.11\times10^{-5}$
442.16	$3.55\times10^{-2}\pm6.81\times10^{-4}$	422.2	$1.57\times10^{-4}\pm1.51\times10^{-4}$
511.16	$4.49\times10^{-2}\pm5.15\times10^{-4}$	514.2	$2.55\times10^{-3}\pm3.59\times10^{-4}$
565.16	$5.40\times10^{-2}\pm8.30\times10^{-4}$	566.2	$3.98\times10^{-3}\pm2.65\times10^{-4}$
613.16	$7.34\times10^{-2}\pm1.04\times10^{-2}$	613.2	$4.56\times10^{-3}\pm3.10\times10^{-4}$
d = 8.7 nm		d = 10.0 nm	
293.7	$6.21\times10^{-4}\pm5.80\times10^{-5}$	296.5	$5.62\times10^{-4}\pm3.90\times10^{-5}$
314.2	$7.39\times10^{-4}\pm1.11\times10^{-4}$	310.4	$6.13\times10^{-4}\pm2.81\times10^{-5}$
354.7	$9.94\times10^{-4}\pm2.49\times10^{-5}$	335.5	$7.07\times10^{-4}\pm3.37\times10^{-5}$
408.2	$1.24\times10^{-3}\pm1.49\times10^{-4}$	367.2	$7.92\times10^{-4}\pm4.33\times10^{-5}$
461.2	$1.72\times10^{-3}\pm1.40\times10^{-4}$	416.2	$1.03\times10^{-3}\pm1.39\times10^{-4}$
508.2	$2.11\times10^{-3}\pm2.28\times10^{-4}$	467.2	$1.48\times10^{-3}\pm3.04\times10^{-5}$
		508.2	$1.71\times10^{-3}\pm1.88\times10^{-4}$
		546.2	$1.97\times10^{-3}\pm1.26\times10^{-4}$
		583.2	$2.40\times10^{-3}\pm1.70\times10^{-4}$
		625.2	$2.75\times10^{-3}\pm1.47\times10^{-4}$

Table 2. Experimentally measured values of the diffusion coefficient D for Pt nanoparticles in nitrogen with mean arithmetic diameter of 6.3, 18.0 and 35 nm and NaCl nanoparticles in air with mean arithmetic diameter 84 nm.

$Pt - N_2$, d = 6.3 nm		$Pt - N_2$, d = 18.0 nm	
T, K	D, cm^2/s	T, K	D, cm^2/s
297.36	$0.00132 \pm 4.35\times10^{-5}$	297.2	$1.84\times10^{-4} \pm 2.06\times10^{-5}$
334.56	$0.00169 \pm 1.83\times10^{-4}$	327.2	$2.71\times10^{-4} \pm 1.47\times10^{-5}$
386.16	$0.00266 \pm 4.58\times10^{-4}$	366.7	$3.38\times10^{-4} \pm 1.52\times10^{-5}$
438.16	$0.0032 \pm 2.74\times10^{-4}$	418.2	$4.79\times10^{-4} \pm 4.95\times10^{-5}$
473.16	$0.00372 \pm 4.95\times10^{-4}$	470.2	$6.09\times10^{-4} \pm 3.67\times10^{-5}$
538.16	$0.00459 \pm 2.17\times10^{-4}$	533.9	$7.83\times10^{-4} \pm 4.00\times10^{-5}$
		597.6	$9.68\times10^{-4} \pm 3.09\times10^{-5}$
$Pt - N_2$, d = 35 nm		$NaCl$ – воздух, d = 84 nm	
T, K	D, cm^2/s	T, K	D, cm^2/s
297.2	$4.67\times10^{-5} \pm 7.98\times10^{-6}$	289.9	$1.03\times10^{-5} \pm 1.39\times10^{-6}$
352.5	$7.92\times10^{-5} \pm 1.23\times10^{-5}$	323.2	$1.2610^{-5} \pm 4.24\times10^{-6}$
407.7	$1.14\times10^{-4} \pm 2.54\times10^{-5}$	371.5	$1.9110^{-5} \pm 1.14\times10^{-6}$
453.2	$1.6610^{-4} \pm 1.17\times10^{-5}$	425.9	$2.6110^{-5} \pm 3.43\times10^{-6}$
504.2	$2.1410^{-4} \pm 7.20\times10^{-5}$	479	$3.0910^{-5} \pm 2.50\times10^{-6}$
553.2	$2.5910^{-4} \pm 1.46\times10^{-5}$	529.5	$3.6710^{-5} \pm 3.16\times10^{-6}$
299.2	$7.12\times10^{-5} \pm 4.64\times10^{-6}$	580.1	$4.2810^{-5} \pm 1.01\times10^{-5}$
341.7	$9.23\times10^{-5} \pm 2.05\times10^{-5}$	615.1	$4.9210^{-5} \pm 8.19\times10^{-6}$
385.2	$1.1710^{-4} \pm 2.85\times10^{-5}$		
455.2	$1.9910^{-4} \pm 5.03\times10^{-5}$		

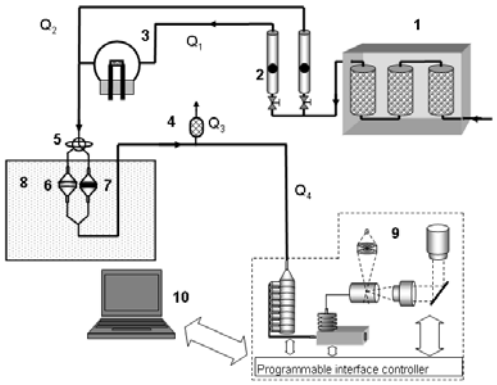

Figure 1. Schematic of the experimental set – up . 1 – gas purification unit "BOG-85", 2 – flow meters, 3 – "hot-wire" generator of WO_x nanoparicles, 4 – HEPA filter, 5 – three-way stopcock, 6 – empty holder, 7 – holder with screens, 8 – thermostat, 9 – NADB, 10 – PC, Q_1, Q_2, Q_3 – career gas flows.

Figure 2. Normalized size distributions of polystyrene latex particles, produced with Colisson-type nebulizer. Size distributions were normalized in a way, that amplitudes of the size distributions maxima had similar values. The types of latex particles has been used: 1 – 41 ± 1.2 nm, 2 – 60 ± 3.6 nm, 3 – 100 ± 5 nm (manufacture's information).

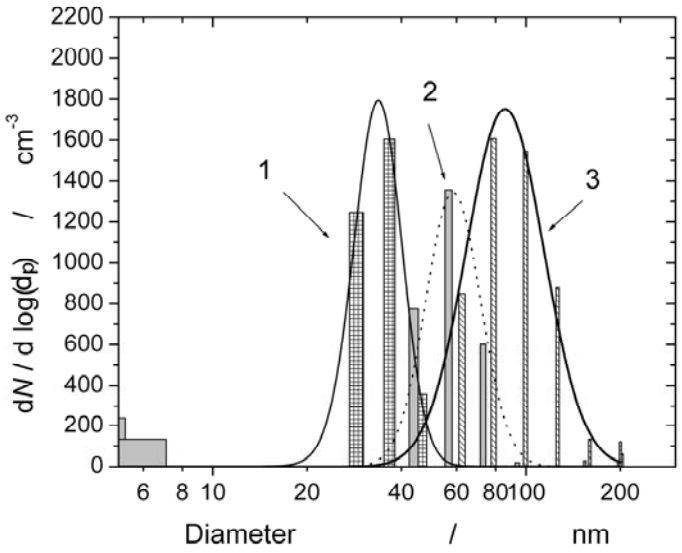

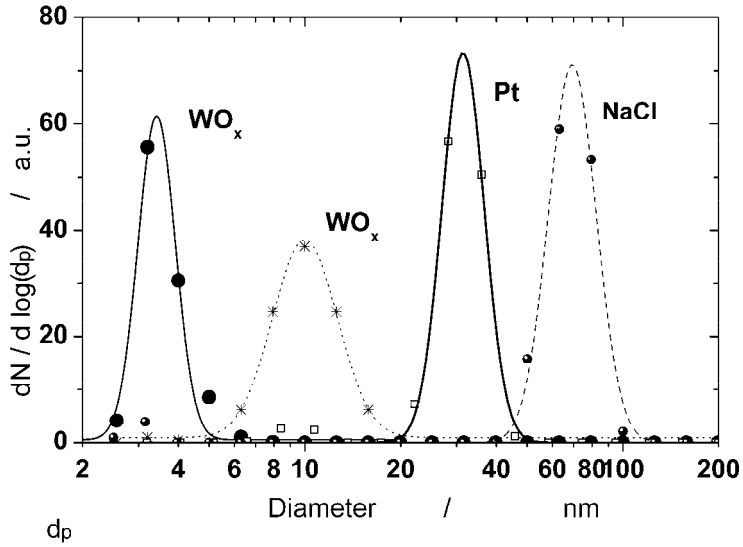

Figure 3. An example of the size distributions of the aerosol particles used in experiments. WO_x – tungsten oxide particles with mean arithmetic diameter of 3.7 and 12.1 nm, Pt – platinum particles with mean arithmetic diameter of 34.5 nm, NaCl – NaCl particles with mean arithmetic diameter of 84 nm. Dots – data, measured with NADB, lines – log-normal fit.

Figure 4. Comparison of the experimentally measured diffusion coefficients (1) for WO_3, Pt and NaCl nanoparticles of different size with calculated values. 2 – CMD-correlation (2), 3 – Baron and Willeke (2001), 4 – experimental correlation (Dubtsov,2005), 5 – Chapman equation (Reid, 1977)

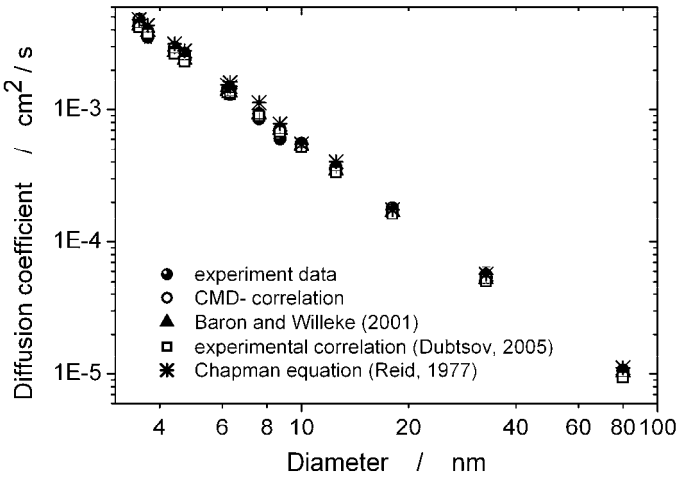

Figure 5. Temperature dependence of the penetration (closed squares) and diffusion coefficient (open circles) for 3.7 nm WO_x nanoparticles in air.

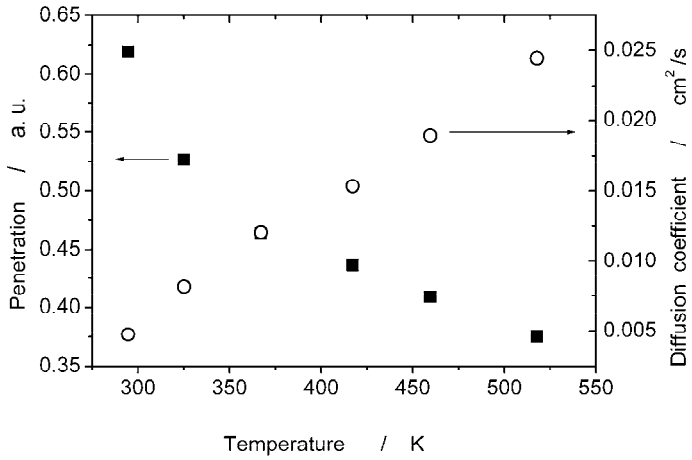

Figure 6. Comparison of the experimentally measured diffusion coefficient temperature dependence of WO_x nanoparticles in air (1) with calculations using CMD-correlation (2) and formulae in (Baron and Willeke, 2001) (3). Line – approximation $D \sim T^{1.7}$. Mean arithmetic diameter of the nanoparticles – 3.5 nm.

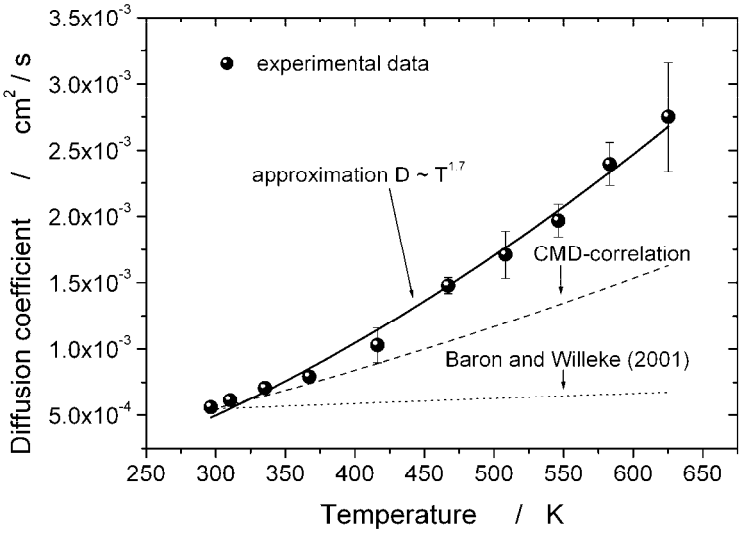

Figure 7. Comparison of the experimentally measured diffusion coefficient temperature dependence of Pt nanoparticles in nitrogen (1) with calculations using CMD-correlation (2) and formulae in (Baron and Willeke, 2001) (3). Line – approximation $D \sim T^{1.55}$. Mean arithmetic diameter of the nanoparticles – 18 ± 2 nm.

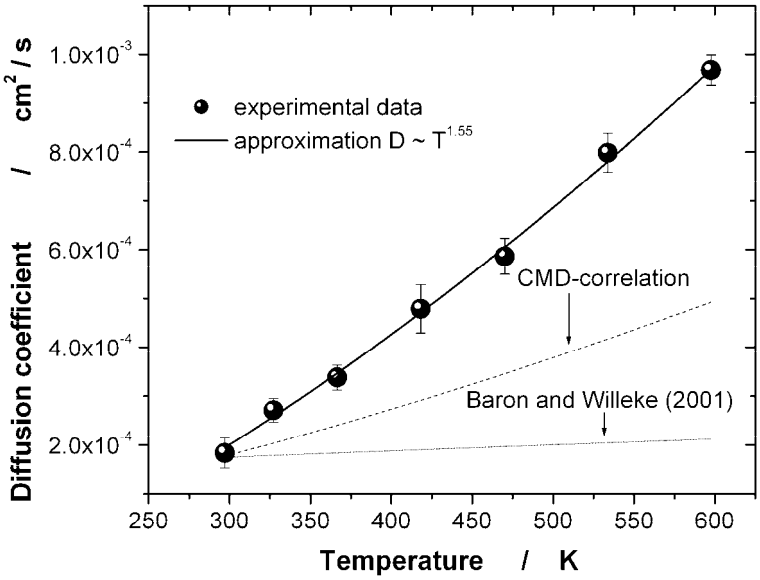

Figure 8. Comparison of the experimentally measured diffusion coefficient temperature dependence of NaCl nanoparticles in air (1) with calculations using CMD-correlation (2) and formulae in (Baron and Willeke, 2001) (3). Line – approximation $D \sim T^{1.40}$. Mean arithmetic diameter of the nanoparticles – 84 ± 6 nm.

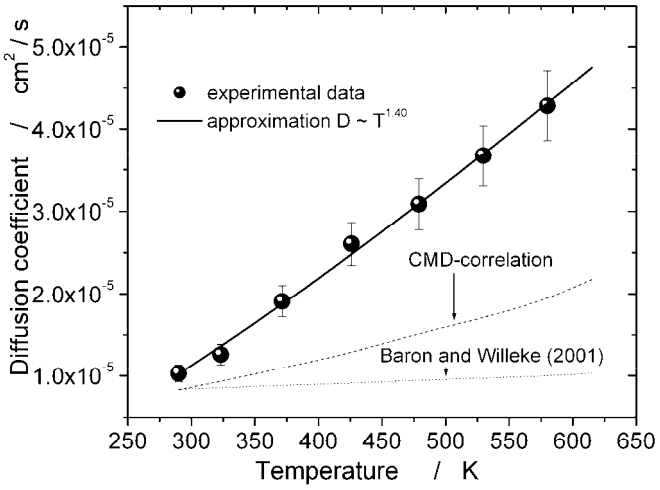

Figure 9. Diffusion coefficient temperature dependence for 6.3 nm WO_x in air (filled circles) and 6.2 nm Pt nanoparticles in N_2 (opened circles).

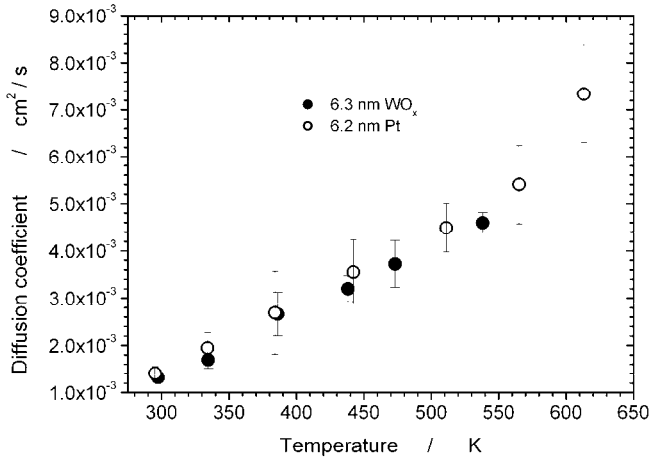

Figure 10. Dependence of the exponent *j* value in the formulae (5.4) on the particle's size.